Diurnal variations of land surface wind speed probability distributions under clear-sky and low-cloud conditions

Yanping He,[1] Adam H. Monahan,[1] and Norman A. McFarlane[2]

Received 20 March 2013; revised 14 May 2013; accepted 16 May 2013.

[1] Long-term 10 min wind tower data and ceilometer backscatter data at Cabauw in the Netherlands provide quantitative information on the influence of low clouds on the diurnal evolution of the near-surface wind speed (NSWS) probability distribution (probability density function), the wind power density (WPD), and their vertical structure in the bottom 200 m of the atmosphere. Under clear-sky conditions, pronounced diurnal cycles are identified in the leading three moments of NSWS as well as WPD and the boundary layer thermal structure in all seasons. When low clouds are present, weaker diurnal cycles with a different vertical structure are observed. Under clear skies, skewness at night is positive within the stable air near the surface but negative above 100 m. In the presence of low clouds, wind speeds are positively skewed and the probability of strong winds is higher associated with a larger geostrophic wind speed. **Citation:** He, Y., A. H. Monahan, and N. A. McFarlane (2013), Diurnal variations of land surface wind speed probability distributions under clear-sky and low-cloud conditions, *Geophys. Res. Lett.*, *40*, doi:10.1002/grl.50575.

1. Introduction

[2] Understanding the diurnal cycle of the near-surface wind speed (NSWS) probability density function (pdf) and its physical controls is important for managing wind energy under future climate change scenarios [*Petersen et al*., 1998; *Burton et al*., 2001], for accurately estimating surface fluxes [*Cakmur et al*., 2004; *Monahan*, 2006], and for providing a simulation benchmark for atmospheric models [*He et al*., 2010, 2012]. The joint influences of large-scale mechanical driving (through the geostrophic winds in the extratropics) and near-surface thermal structure on boundary layer turbulence exercise an important control on fluxes of mass, energy, and momentum between the free atmosphere and the underlying land surface. The thermal structure is strongly influenced by the existence of low-level cloudiness (LLC) above the boundary layer top [*Stull*, 1988]. In earlier work, the surface wind speed pdf has been studied based on 3734 surface weather stations across the globe without distinction between conditions of clear and cloudy skies [*He et al*., 2010; *Monahan et al*., 2011]. These distributions are characterized by a Weibull-like daytime pdf and a nighttime pdf with a skewness that consistently exceeds the predicted value from a Weibull distribution. Current state-of-the-art regional climate models (RCMs) and reanalysis products fail to capture this observed diurnal variation of NSWS pdf over North America [*He et al*., 2010]. *Monahan et al*. [2011] demonstrated that this diurnal cycle in the NSWS pdf is characteristic of a shallow atmospheric layer with a depth of a few tens of meters. The general features of the diurnal variation of the leading three NSWS moments and their fine vertical structures between 10 m and 200 m observed at Cabauw have been simulated in a single-column model study neglecting the influence of moist physics using a diagnostic turbulent kinetic energy scheme and a simple stochastic wind model representing planetary boundary layer (PBL) top intermittent turbulence [*He et al*., 2012].

[3] In the present study, we extend and continue these previous analyses by providing a picture of the observed diurnal variations of NSWS pdf and its vertical structure under both clear-sky and low-level cloudy-sky conditions at Cabauw. Observed relationships among the NSWS pdf, near-surface thermal structure, low-level clouds, and surface geostrophic winds are also addressed for day and night and in all seasons. The data considered in this study are described in section 2; the observed diurnal variations of NSWS moments, the theoretical wind power density (WPD), the near-surface thermal structure, and surface geostrophic winds are presented and discussed in section 3; and a summary and conclusions follow in section 4.

2. Data Description

[4] To investigate the pdf of near-surface winds under clear-sky and cloudy-sky conditions, wind, temperature, and cloud information were obtained for the period from January 2007 to December 2011 from the Cabauw Experimental Site for Atmospheric Research, which maintains a 213 m tall tower at Cabauw (528°N, 4.98°E) in the western Netherlands (http://www.cesar-database.nl/). The wind tower is located in open, flat pastureland with few nearby wind breaks, such as houses or trees. Validated observations of 10 min averaged wind (speed and direction) and temperature were obtained from 2007 to 2011 at heights of 10, 20, 40, 80, 140, and 200 m. Hourly surface geostrophic wind data are based on a 2-D polynomial fit to surface pressure observations within a 75 km radius of Cabauw, from which a gradient is calculated.

[5] The climatological wind speed pdf will be described by the first three statistical moments (mean, standard deviation (hereafter "std"), and skewness; discussed in detail in *Monahan* [2006]). The first two of these moments are

[1]School of Earth and Ocean Sciences, University of Victoria, Victoria, British Columbia, Canada.
[2]Canadian Centre for Climate Modelling and Analysis, University of Victoria, Victoria, British Columbia, Canada.

Corresponding author: Y. He, School of Earth and Ocean Sciences, University of Victoria, PO Box 3065 STN CSC, Victoria, BC V8W 3V6, Canada. (yhe@uvic.ca)

0094-8276/13/10.1002/grl.50575

Table 1. Frequencies of Clear-Sky (CLR) and Low-Level Cloudiness (LLC) Conditions (See Text for Definitions) in Four Seasons During Day (7 A.M. to 7 P.M.) and Night (7 P.M. to 7 A.M.) From 2007 to 2011 at Cabauw

Season	Day (CLR, LLC)	Night (CLR, LLC)
DJF	(24%, 46%)	(26%, 42%)
MAM	(40%, 24%)	(46%, 18%)
JJA	(29%, 24%)	(39%, 19%)
SON	(30%, 32%)	(36%, 27%)

measures of wind speed magnitude (the average and the variability, respectively); in contrast, the skewness is a measure of the shape of the wind speed distribution. These moments are estimated separately for each data subset (time of day, season, and sky condition (clear versus cloudy)) using 10 min wind, temperature, and cloud data. There are up to 1000 wind records for each subset during the study period. The cloud information data set contains backscatter profiles and system status signals from a CT75 ceilometer with 30 s time resolution (CT75 ceilometer backscatter data version 1.0). Operationally retrieved cloud base heights are included in these data (up to three levels). From these data, we determined the sky condition based on the frequency of observed cloud bases (between 0 and 20 per 10 min) and the height of the cloud base. The 10 min wind and temperature records are classified into three categories: "clear-sky" cases for which $N_{cb} = 0$ (the number of observed cloud bases per 10 min), persistent low-level cloudiness cases (hereafter "low-level cloudiness (LLC)") for which $N_{cb} \geq 10$ and the height of the lowest cloud base is within 1.5 km of the surface, and partial clouds cases (all other cases). Analyses carried out without consideration of sky conditions will be referred to as "all-sky." The cloud data record is continuous, but there are a few gaps (less than 10% of the record) where no cloud data are available. The corresponding wind observations for these

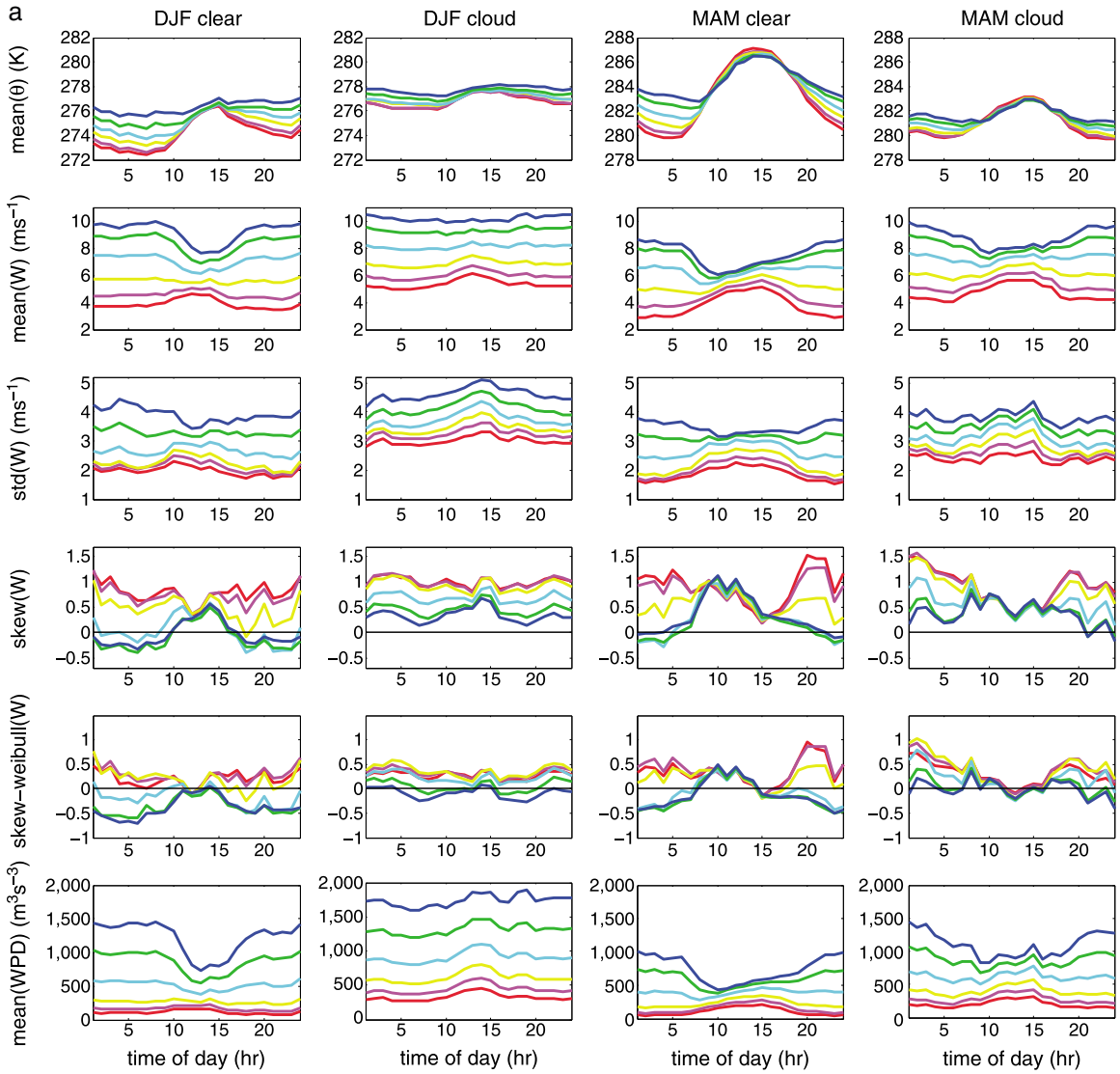

Figure 1. (a) Diurnal variations of potential temperature (first row), mean (second row), standard deviation (std) (third row), skewness of wind speed(fourth row), skewness excess of wind speed (fifth row), and mean wind power density (WPD) (sixth row) at six wind tower levels (10 m, red; 20 m, pink; 40 m, yellow; 80 m, cyan; 140 m, green; and 200 m, blue) under clear-sky (odd columns) and LLC (even columns) conditions at the Cabauw site for DJF and MAM from 2007 to 2011. (b) As in Figure 1a but for JJA and SON.

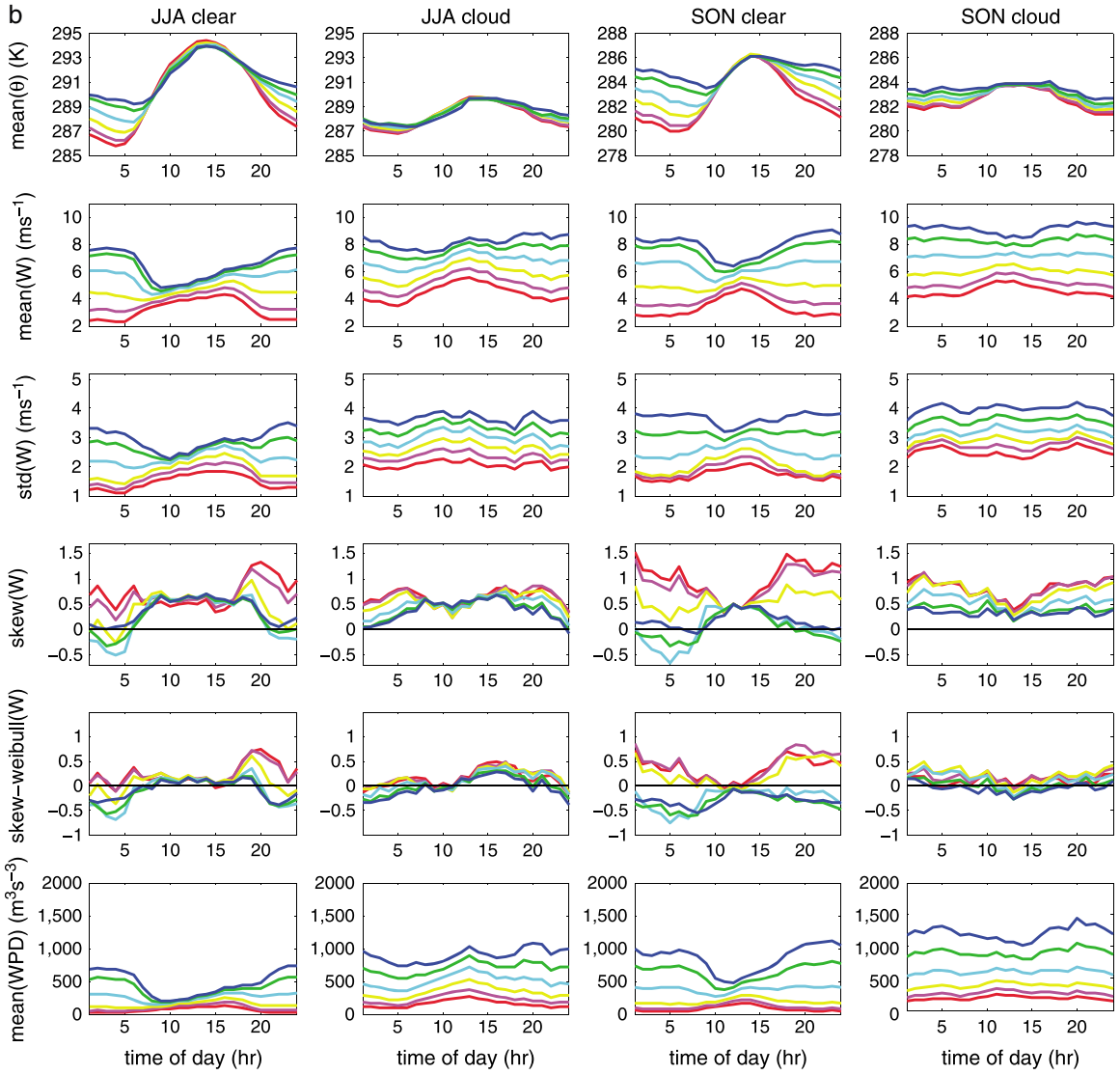

Figure 1. (continued)

periods were not considered for calculations of wind statistics. In this study, we consider NSWS pdf variability under the contrasting clear-sky and LLC cases. The results of these analyses are not qualitatively altered if the NSWS pdf is computed based on slightly different criteria for the LLC case. Table 1 shows the frequencies of these two sky cases in four seasons during daytime (from local 7 A.M. to 7 P.M.) and nighttime (from local 7 P.M. to 7 A.M.) from 2007 to 2011. In winter, a greater frequency of LLC conditions (>40%) is found at both day and night. In the rest of a year, the clear-sky frequency is generally higher than that of LLC (particularly at night).

3. Results

[6] The extratropical NSWS pdf is influenced by large-scale geostrophic wind variations and the thermal structure of the boundary layer over local land surface [*Barthelmie et al.*, 1996; *Dai and Deser*, 1999; *Monahan et al.*, 2011; *He et al.*, 2010, 2012], which can be significantly different under clear-sky and cloudy-sky conditions. The observed diurnal variations of the mean, std, skewness, and skewness excess of NSWS at six wind tower vertical levels are shown under clear-sky and LLC conditions for December-January-February (DJF) and March-April-May (MAM) (Figure 1a) and June-July-August (JJA) and September-October-November (SON) (Figure 1b) during the period from 2007 to 2011. Also shown is the diurnal evolution of the mean potential temperature (θ) and the theoretical WPD (given by the mean cubed wind speed) at each altitude. The skewness excess is defined as the difference between the observed skewness and that of a best fit Weibull distribution [*Monahan et al.*, 2011].

[7] It is evident from Figure 1 that the clear-sky thermal structure is characterized by a well-mixed θ within an active daytime buoyancy-driven PBL and a strong nocturnal temperature inversion capping a stable PBL. The diurnal evolution of the mean and std of clear-sky NSWS from the surface to 80 m exhibits the canonical pattern of NSWS [*Dai and Deser*, 1999], with daily maxima around noon in the unstable PBL and daily minima within the general quiescent shallow stable PBL at night. Diurnal variations of the mean and std are reversed between 100 m and 200 m with the larger values at night likely associated with the

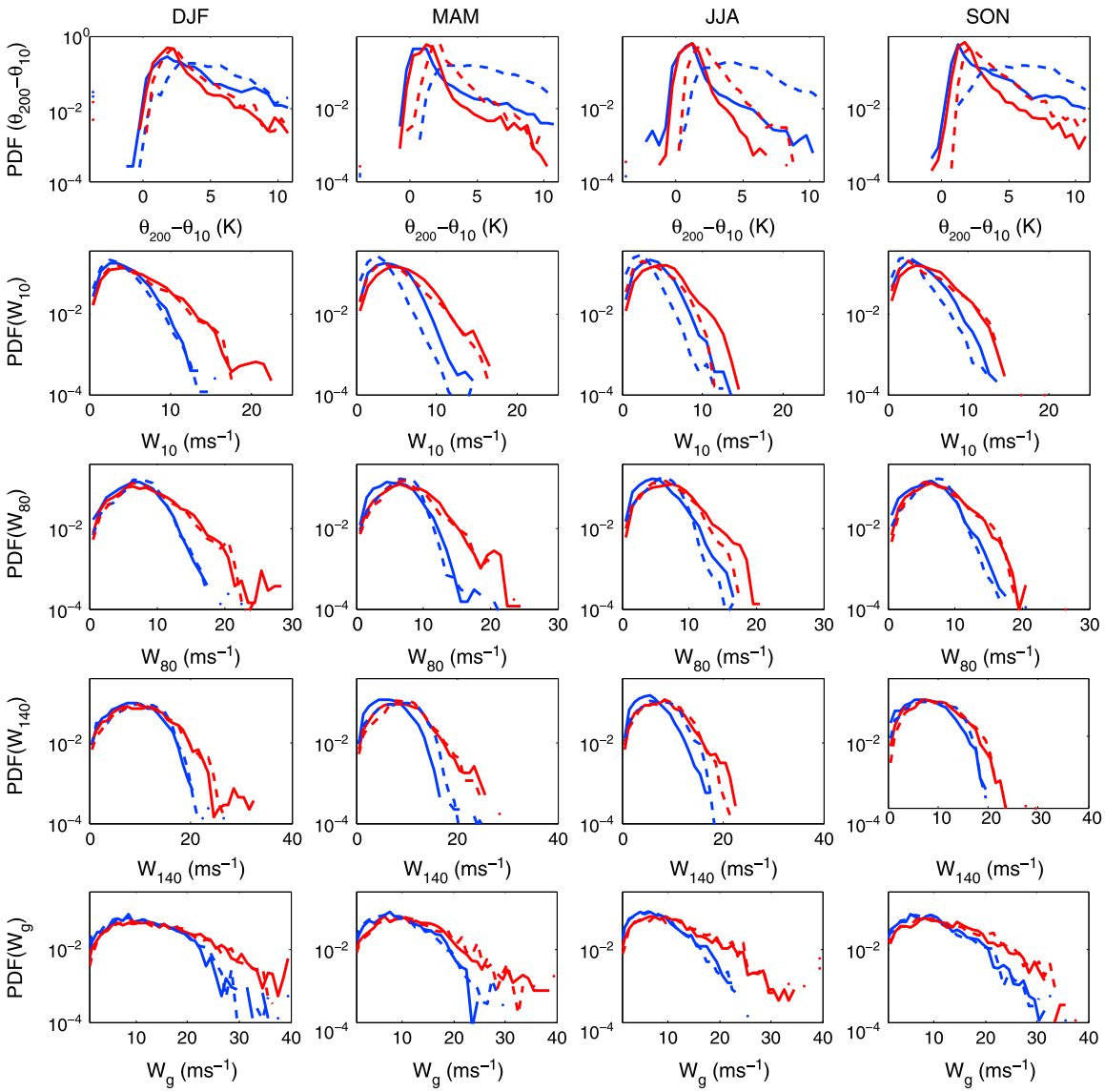

Figure 2. The pdf (logarithmically scaled) of potential temperature stratification between 200 m and 10 m ($\theta_{200} - \theta_{10}$); wind speed at 10 m ($W_{10}$), 80 m ($W_{80}$), and 140 m ($W_{140}$); and the surface geostrophic wind speed (W_g) during daytime (7 A.M. to 7 P.M.) (solid) and nighttime (7 P.M. to 7 A.M.) (dashed) under clear sky (blue) and LLC (red) at the Cabauw site for each of the seasons from 2007 to 2011.

development of a low-level jet under fair weather conditions [*Baas et al.*, 2009]. Over the course of the seasons, the mean and std of NSWS across these altitudes are largest in DJF and smallest in JJA. Daytime vertical gradients in these quantities are smallest in JJA under clear-sky conditions when the land surface buoyancy fluxes are the largest, but become larger in DJF when the land surface is cold and the surface buoyancy flux is smaller. At night, the clear-sky mean and std of NSWS show large vertical shears in all seasons associated with the decoupling between surface winds and those above when a strong capping temperature inversion forms above a very shallow stable PBL. The diurnal variation of NSWS skewness under clear skies is similar to that under all-sky conditions [*Monahan et al.*, 2011; *He et al.*, 2012] with a positively skewed daytime NSWS pdf and a reversal in nocturnal NSWS skewness from positive within the stable layer to negative above 100 m. During the day, the wind speeds are close to the Weibull distribution throughout the bottom 200 m, while at night, the skewness excess is positive in the bottom 80 m and negative above that.

[8] The observed diurnal evolution of the NSWS pdf and the boundary layer thermal structures are significantly different in the presence of low clouds (Figure 1). The LLC mean and std of NSWS show a much smaller diurnal variation and a larger vertical gradient during the daytime across the bottom 200 m in all seasons, which is consistent with the observed much weaker diurnal amplitude of θ and a near-neutral PBL in both day and night. Under LLC conditions, the NSWS pdf is generally found to be reasonably well represented by the Weibull distribution in both day and night. The skewness demonstrates a weaker diurnal variation than that under clear skies and is positive throughout the bottom 200 m.

[9] The logarithmically scaled pdf of NSWS at 10 m, 80 m, and 140 m is shown in Figure 2 under clear-sky and LLC conditions in both day (7 A.M.–7 P.M.) and night (7 P.M.–

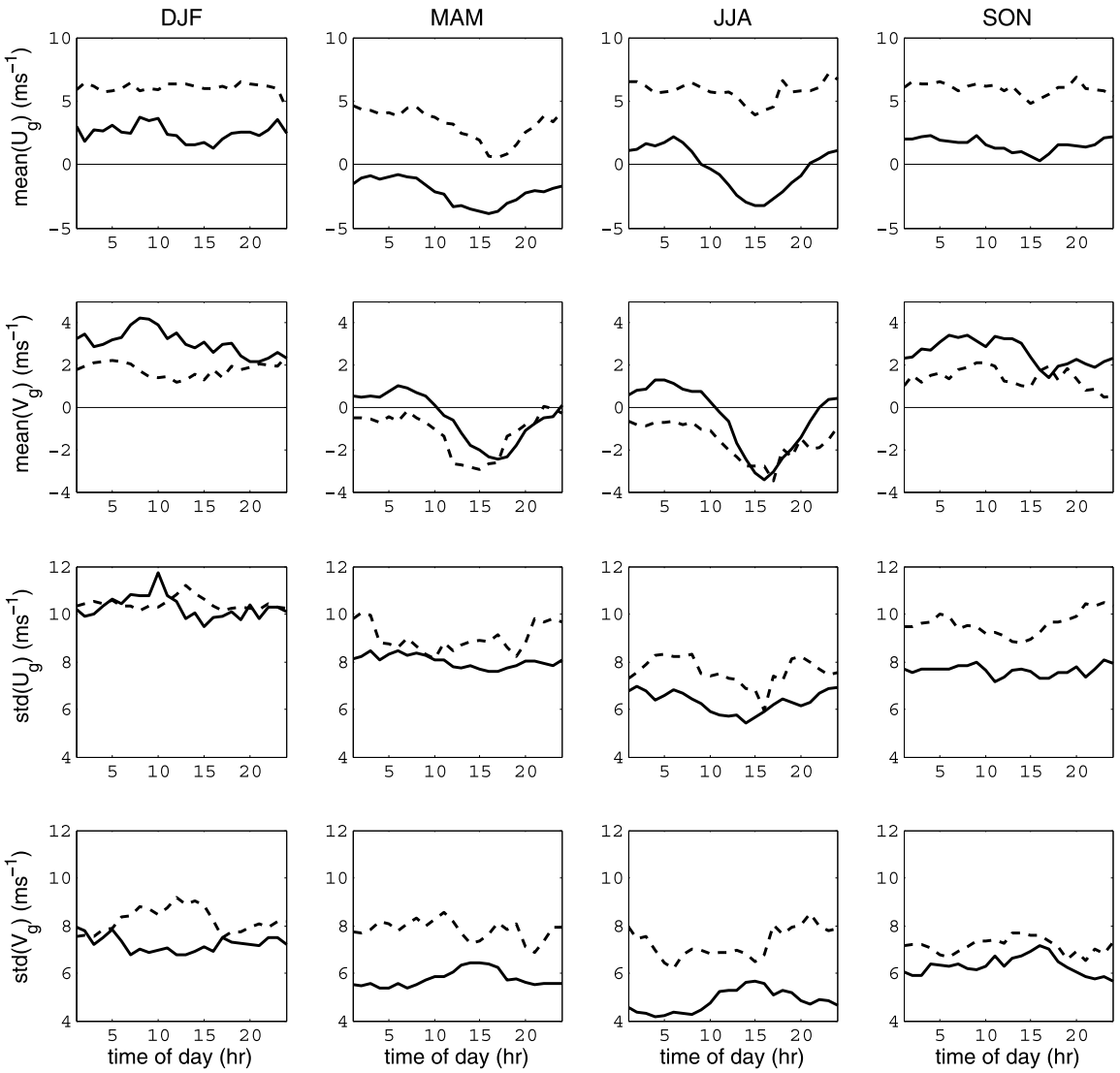

Figure 3. Diurnal variations of the mean and standard deviation of the surface geostrophic wind components U_g and V_g under clear-sky (solid) and LLC (dashed) conditions at the Cabauw site for all seasons from 2007 to 2011.

7 A.M.) for each of the four seasons. Also shown are diurnal variations of the pdf of near-surface potential temperature stratification $\Delta\theta$ (defined as $\theta_{200} - \theta_{10}$) and surface geostrophic wind speed (W_g). Under LLC conditions, the $\Delta\theta$ pdf is relatively narrow in both day and night, with a peak corresponding to a weakly stratified state. In contrast, the $\Delta\theta$ pdf differs substantially between day and night under clear skies. During the day, the $\Delta\theta$ distribution is narrow with a near-neutral peak; at night, the $\Delta\theta$ distribution is broad, with a long tail toward conditions of strong positive (statically stable) $\Delta\theta$. The NSWS pdf is strongly influenced by near-surface $\Delta\theta$ [*He et al.*, 2010; *Monahan et al.*, 2011] and shows different diurnal evolution under the two sky conditions. At 10 m, 80 m, and 140 m, the NSWS pdf differences between day and night are generally smaller than the differences between clear-sky and LLC conditions. In all seasons and at all vertical levels, the LLC NSWS is characterized by higher probability of stronger wind speeds. This is also observed to be true of W_g at Cabauw.

[10] The NSWS distribution is strongly influenced by the W_g distribution [*Petersen et al.*, 1998; *He et al.*, 2012], which itself depends on both the mean and the variability of the vector components of the geostrophic flow [*Monahan*, 2012]. Figure 3 displays the diurnal variations of the mean and std of the surface geostrophic wind components U_g and V_g under clear sky and LLC for the four seasons. Under clear-sky conditions, surface geostrophic winds from the southwest dominate during DJF and SON. In MAM and JJA, the direction changes during the morning hours under LLC and reverses under clear-sky conditions. The predominance of near-surface geostrophic flows from the northeast quadrant in the summer is consistent with pressure patterns with relatively low pressure over the European continent adjacent to the North Sea. The actual near-surface wind directions (not shown), although exhibiting considerable variability, are predominantly from the northwest quadrant in the afternoon for clear-sky conditions. These features are consistent with the occurrence of sea breeze circulations that may extend as much as 100 km inland from the North Sea on clear summer afternoons [*Tijm et al.*, 1999]. Under LLC conditions, U_g and V_g show large mean values and large variability associated with synoptic storm activity. This

observation is consistent with increased mechanical driving under LLC conditions as shown in Figure 2: The surface W_g pdfs are observed to extend to larger wind speed values under LLC conditions relative to that clear skies. Furthermore, the mean U_g under LLC is from the west in all seasons, with associated large-scale moisture transport from the ocean, which helps maintain the low-level clouds.

[11] The wind power density is proportional to the third power of wind speed and is uniquely determined by the first three moments of the NSWS [*Hennessey*, 1977]. The diurnal variation of mean WPD at six vertical levels between 10 m and 200 m is presented in Figure 1. The skewness variation of NSWS typically accounts for less than 10% of the mean WPD [*He et al*., 2010], so the diurnal variation of mean WPD generally follows those of the mean and std of the NSWS pdf with large diurnal amplitudes only under clear-sky conditions. The clear-sky mean WPD reaches a daily maximum around noon in the bottom 40 m and a daily maximum at night around the wind turbine hub height range between 80 m and 200 m. At each altitude, it reaches its seasonal maximum in DJF and its seasonal minimum in JJA. The clear-sky daytime WPD is not sensitive to the height of the wind turbine because near-surface winds are well mixed. However, the LLC WPD shows a much smaller diurnal cycle and presents a large vertical gradient in both day and night. In particular, the daytime mean WPD at 200 m can be up to 6 times as large as that at 20 m under LLC conditions.

4. Summary and Conclusions

[12] Long-term observations of near-surface wind, temperature, and clouds with 10 min resolution have been used in this study to characterize the NSWS pdf and its vertical structure under conditions of clear and cloudy skies at Cabauw, Netherlands. Previous studies at this location [e.g., *Monahan et al*., 2011] considered the diurnal evolution of the pdf without considering forcing variations associated with clouds; the present study provides the first quantitative demonstration that the NSWS pdf is significantly different between clear-sky and cloudy-sky conditions. The main findings can be summarized as follows.

[13] 1. Diurnal variations of the mean and std of NSWS demonstrate a clear relationship with the diurnal evolution of the boundary layer thermal structure in all seasons, both of which are strongly influenced by the presence of low clouds.

[14] 2. The clear-sky NSWS skewness is positive (and greater than the best-fit Weibull variable) in a shallow nocturnal PBL below 50 m but negative in the nocturnal jet level above 100 m. Under LLC conditions, the NSWS pdf is found to be positively skewed and be closely approximated by the Weibull distribution at all altitudes and times of day. Furthermore, the LLC NSWS has higher probability of strong winds associated with stronger driving surface geostrophic winds.

[15] 3. Diurnal variations of wind power density mainly follow the leading two moments of NSWS variations. The mean WPD is not sensitive to height (due to the well-mixed mean and std of NSWS) within the clear-sky daytime PBL but shows significant vertical gradients at night under clear sky and for both day and night under LLC conditions.

[16] The data considered in this study are from a single midlatitude site in a region with relatively homogeneous surface conditions. In this idealized setting, the diurnal variations in winds and temperature are dominated by radiative and turbulent fluxes in the vertical [e.g., *Monahan et al*., 2011; *He et al*., 2012]. The results presented in this study are expected to be relevant to other locations to the extent that the same physical processes are dominant. Where other processes (e.g., horizontal transports) become important or the vertical transports are qualitatively different (e.g., because of different cloud climatology), the diurnal evolution of winds and temperature may accordingly differ. A detailed investigation of this lower atmospheric variability in a broad range of physical settings is complicated by the absence of tall towers with long, high-resolution records such as that at Cabauw. Nevertheless, the physically consistent picture emerging from consideration of these data provides a baseline understanding of the influence of low clouds on the diurnal cycles of lower atmospheric wind and temperature.

[17] In summary, this work provides quantitative information on the influence of low clouds on the diurnal evolution of NSWS, WPD, and their vertical structure in the bottom 200 m of the atmosphere. Knowledge from this study is essential for understanding the diurnal variations of not only mean winds but also extreme winds near the surface at 10 m and at wind turbine hub heights above 80 m under both clear-sky and low-cloud conditions, which has important applications for wind energy and wind risk assessment and management. RCMs and global climate models have been extensively used for future projections of surface mean and extreme wind event change and wind power estimation [*Pryor et al*., 2005, 2012; *McInnes et al*., 2011]. A major uncertainty for these future projections comes from model limitations associated with their physical parameterization schemes. This study provides a basis for better assessing and improving schemes that represent the effects of boundary layer processes in such models.

[18] **Acknowledgments.** This research is supported by the NSERC CREATE Training Program in Interdisciplinary Climate Science. The surface geostrophic data were provided by Fred Bosveld at The Royal Netherlands Meteorological Institute, and the tower data were provided by the Cabauw Experimental Site for Atmospheric Research (CESAR). A. H. Monahan gratefully acknowledges support from the Natural Sciences and Engineering Research Council of Canada. The authors thank two reviewers for the helpful comments.

[19] The Editor thanks two anonymous reviewers for their assistance in evaluating this paper.

References

Baas, P., F. C. Bosveld, H. Klein Baltink, and A. A. M. Holtslag (2009), A climatology of nocturnal low-level jets at Cabauw, *J. Appl. Meteorol. Climatol.*, *48*, 1627–1642.

Barthelmie, R. J., B. Grisogono, and S. C. Pryor (1996), Observations and simulations of diurnal cycles of near-surface wind speeds over land and sea, *J. Geophys. Res.*, *101*(D16), 21,327–21,337.

Burton, T., D. Sharpe, N. Jenkins, and E. Bossanyi (2001), *Wind Energy Handbook*, 617 pp., John Wiley, Chichester, UK.

Cakmur, R. V., R. L. Miller, and O. Torres (2004), Incorporating the effect of small-scale circulations upon dust emission in an atmospheric general circulation model, *J. Geophys. Res.*, *109*, D07201, doi:10.1029/2003JD004067.

Dai, A., and C. Deser (1999), Diurnal and semidiurnal variations in global surface wind and divergence fields, *J. Geophys. Res.*, *104*(D24), 31,109–31,125, doi:10.1029/1999JD900927.

He, Y., A. H. Monahan, C. G. Jones, A. Dai, S. Biner, D. Caya, and K. Winger (2010), The probability distribution of land surface wind speed

over North America, *J. Geophys. Res.*, *115*, D04103, doi:10.1029/2008JD010708.

He, Y., N. McFarlane, and A. H. Monahan (2012), The influence of boundary layer processes on the diurnal variation of the climatological near-surface wind speed probability distribution over land, *J. Clim.*, *25*, 6441–6458.

Hennessey, J. P., Jr. (1977), Some aspects of wind power statistics, *J. Appl. Meteorol.*, *16*, 119–128.

McInnes, K. L., T. A. Erwin, and J. M. Bathols (2011), Global climate model projected changes in 10 m wind speed and direction due to anthropogenic climate change, *Atmos. Sci. Lett.*, *12*, 325–333.

Monahan, A. H. (2006), The probability distribution of sea surface wind speeds. Part I: Theory and sea winds observations, *J. Clim.*, *19*, 497–520.

Monahan, A. H. (2012), Can we see the wind? Statistical downscaling of historical sea surface winds in the subarctic northeast Pacific, *J. Clim.*, *25*, 1511–1528.

Monahan, A. H., Y. He, N. McFarlane, and A. Dai (2011), The probability distribution of global land surface wind speed, *J. Clim.*, *24*, 3892–3909.

Petersen, E. L., N. G. Mortensen, L. Landberg, J. Hojstrup, and H. P. Frank (1998), Wind power meteorology part I: Climate and turbulence, *Wind Energy*, *1*, 25–45.

Pryor, S. C., R. J. Barthelmie, and E. Kjellstrom (2005), Potential climate change impact on wind energy resources in northern Europe: Analyses using a regional climate model, *Clim. Dyn.*, *25*, 815–835.

Pryor, S. C., R. J. Barthelmie, and J. T. Schoof (2012), Past and future wind climates over the contiguous USA based on the North American Regional Climate Change Assessment Program model suite, *J. Geophys. Res.*, *117*, D19119, doi:10.1029/2012JD017449.

Stull R. B. (1988), *An Introduction to Boundary Layer Meteorology*. Kluwer Academic Publishers, chap. 13, Kluwer Acad, the Netherlands.

Tijm, A. B. C., A. J. van Delden, and A. A. M. Holtslag (1999), The inland penetration of sea breezes, *Contrib. Atmos. Phys.*, *72*(4), 317–328.